2018

# Experimental Study of Condensation Heat Transfer of R134a on Oil-infusion Surfaces

Hongqing Jin
*University of Illinois at Urbana-Champaign, United States of America*, hj8@illinois.edu

Yuchen Shen
*University of Illinois at Urbana-Champaign, United States of America*, yshen51@illinois.edu

Wentao Ni
*Department of Mechanical Science and Engineering, University of Illinois at Urbana-Champaign, USA*, wni5@illinois.edu

Xiaofei Wang
*University of illinois at urbana champaign, United States of America*, wangxf@illinois.edu

# Experimental Study of Condensation Heat Transfer of R134a on Oil-infused Metal Foams

Hong-Qing JIN, Yuchen SHEN, Wentao NI, Xiaofei WANG*

Department of Mechanical Science and Engineering,
University of Illinois at Urbana-Champaign,
Urbana, IL, USA
E-mail: wangxf@illinois.edu

* Corresponding Author

## ABSTRACT

The condensation process of refrigerants has crucial influence on the efficiency of heating, ventilation, air conditioning and refrigerating systems. Recent research has shown that the use of nanostructured surface with lubricant infusion can enhance condensation heat transfer for low surface tension liquids, which have similar properties with refrigerants. R134, as a highly applied refrigerant, was employed to conduct condensation experiments at a saturation state within a pressure chamber. We also introduced lubricant-infused metal foam surfaces to explore their performance in heat transfer enhancement. A vertical plate surface was cooled by circulate chiller and exposed to the saturated vapor, while the heat flux as well as heat transfer coefficient were calculated based on the one-dimensional heat conduction model. The boundary conditions were well controlled, and the repeatability of the condensation experiment were validated through parallel tests. The preliminary results showed that compared to the pure copper surface, the heat transfer coefficient is increased by 102% and 53% using oil-infused nickel foam and copper foam.

## 1. INTRODUCTION

Refrigerants, as the working fluids, are widely used in heating, ventilation, air conditioning and refrigeration systems (HAVC&R). The condensation heat transfer of refrigerants on surfaces has crucial influence on the efficiency of HVAC&R systems. Many efforts have been dedicated to surfaces modification to promote dropwise condensation for heat transfer enhancement (Li *et al*., 2007), of which most studies are devoted to the condensation of water (Vemuri and Kim, 2006; Chen *et al.*, 2011; Rahman and Jacobi, 2013; Miljkovic and Wang, 2013; Hu and Tang, 2014; Wen *et al.*, 2017). However, unlike water in the atmosphere, refrigerants have much lower surface tension under most working conditions. The condensation and wetting behavior of the low surface tension fluids are different from water (Rose, 2004; Liu and Kim, 2014; Li and Hrnjak), and the condensation of refrigerants on metal surfaces spreads as a thin film due to the big surface energy difference between metal and refrigerants. Surfaces coated with low energy materials (plasma polymer) were also examined during refrigerants condensation, and the heat transfer performance was found deteriorated due to a low thermal conductivity of the coating (Gebauer *et al*, 2013). The slippery lubricant infused porous surface (SLIPS) shows the ability of liquid condensate rapidly breaking down from the interface (Vogel *et al.*, 2013), which could promote antifouling performance (Xiao *et al*., 2013), anti-icing performance (Yu and Jacobi, 2015). Rykaczewski *et al*. (2014) experimentally investigated the condensation process of multiple low surface tension fluids on a lubricant-infused surface (LIS). The condensation heat transfer coefficient (HTC) of hexane, pentane and ethanol on LIS is 3, 4 and 8 times higher than the unimpregnated nanotexture surface. Later, Preston *et al*. (2018) also reports the condensation HTC of toluene on a LIS tube surface is enhanced by 450%. However, the depletion of lubricant by the shear force of liquid condensate would lead to a failure in maintaining a high HTC during condensation.

Metal foams are introduced for their good mechanical properties, large surface area and high porosities. The common problem using lab created nanostructured surface is that their durability and mechanical strength are relatively low for industrial application. During condensation, the large thermal conductivity of metal can enhance heat conduction through the ligaments. In addition, metal foams, manufactured by metal powder sintering, can have an open-celled structure with a minimum pore size of 20 μm, which can be applied to hold low surface tension lubricant within the pores.

In this work, the condensation process of R134a on lubricant-infused metal foam surfaces was experimentally investigated. The heat flux and HTC were measured based on the one-dimensional heat conduction, while the formation of the condensate was observed via a high-speed camera. The condensation of R134a on bare copper surface, metal foam (copper foam and nickle foam) and metal foam with oil infused has been conducted and the HTC has been measured.

## 2. EXPERIMENTAL

### 2.1 Sample preparation

The open-cell copper and nickel foams were supplied by a specialized company. The metal foams, with the thickness of 1 mm, were water cut into the rectangle pieces with the dimension of 1.5 × 3.6 $cm^2$. The nominal pore size is 50 μm for copper foam, and 40 μm for nickel foam. The pore structure was observed under a scanning electron microscope (SEM) in three magnifications, as shown in Fig 1. The porosities of metal foams were determined based on the foam bulk and pure metal density. The samples were rinsed by acetone and distilled water using ultrasonic cleaner, then dried in a sealed container with desiccant.

The Krytox 1506 lubricant oil was adopted to prepare a liquid-infused porous surface. The oil was chosen for its immiscibility to water, ethanol, isopropyl alcohol and multiple organic liquid (Sett, 2017), which have similar properties to R134a. The metal foams were first immerged into the Krytox 1506 to be fully saturated with oil by the capillary force, and then placed vertically to remove the extra oil.

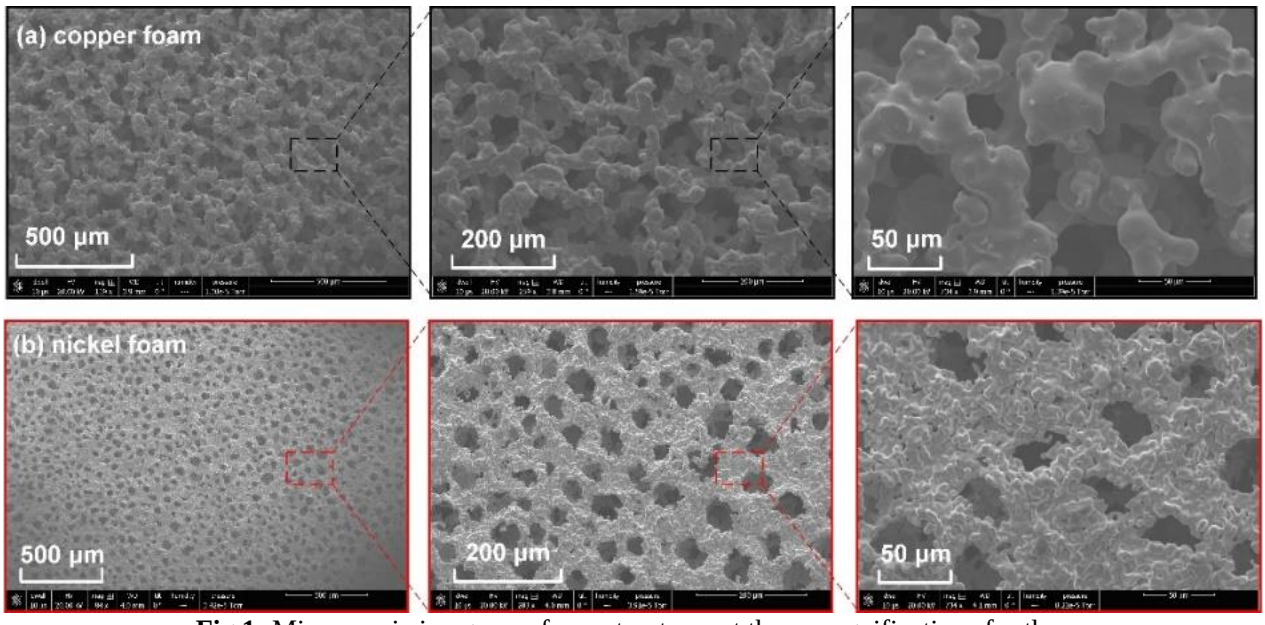


**Fig 1:** Microscopic images on foam structures at three magnifications for the (a) copper foam and (b) nickel foam

### 2.2 Experimental setup and procedure

The condensation of R134a under saturated condition were conducted within a cubic steel chamber at ambient temperature, as shown in Fig 2. The experimental setup consists of the pressure chamber, a chiller (stability ±0.1 °C) for cooling the surface temperature, two water baths (one for heating the cold plate to evaporate the liquid on the

sample surface after the condensation and the other for the chamber temperature and pressure control during the condensation), a data acquisition system, and a high-speed camera. Within the pressure chamber, the cold plate served as an isothermal cooling boundary for condensation tests, and the hot plate connected to one of the water bath to maintain the internal temperature and pressure at a steady state. Two copper blocks (2.0 × 2.5 × 4.6 $cm^3$) were fixed to the vertically placed cold plate, as illustrated in Fig 2 (a). The sample was attached on the top surface of each copper block. Two K type thermocouples (TCs), calibrated to ±0.1°C, were embedded in the center of each copper block. Another TC was fixed near the top of the samples to measure the R134a vapor temperature. The pressure change during condensation was also monitored by the pressure transducer (accuracy ±0.10%). The TC and pressure transducer readings were recorded by the DAQ system with a sample rate of 2 Sps. All the lateral surfaces of copper block were covered by thermal insulation materials to create a one-dimensional heat conduction process.

The chamber was first vacuumed, then charged by a heated container with R134a to the saturated condition at ambient temperature. The condensation process was triggered by turning on the chiller circulation. Condensation of R134a on the metal foams (with/without infused oil), as well as bare copper surfaces were observed. At the meantime, the temperatures at different locations and vapor pressure were measured.

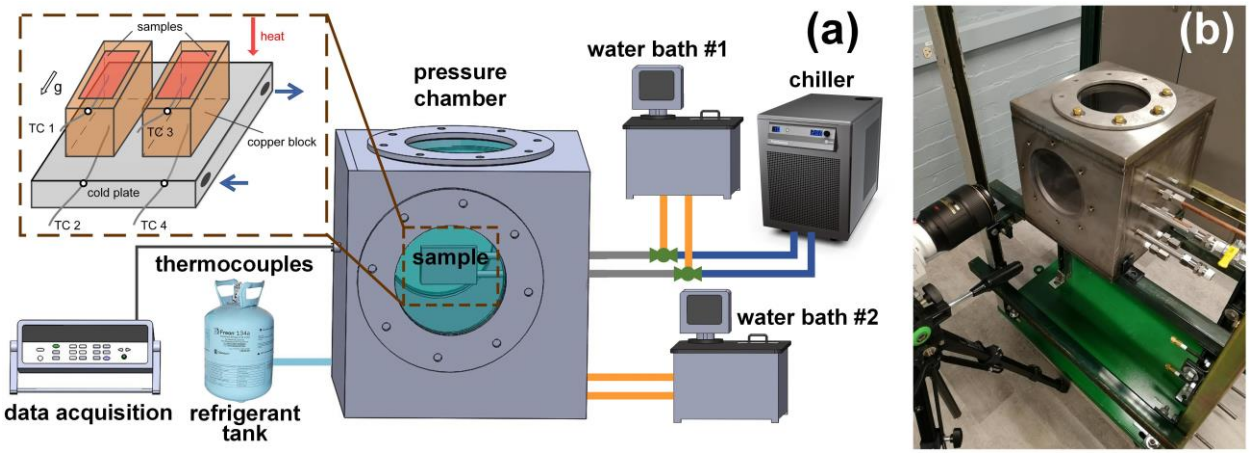


**Fig 2**: Photographs showing (a) the schematic diagrams for R134a condensation as well as the TCs location, and (b) the real experimental facility.

## 3. RESULTS AND DISCUSSION

### 3.1 Properties of metal foams

With the dimensions and mass of the metal foam measured, the bulk density of metal foams ($\rho_{bulk}$) can be determined by its volume and weight, accordingly, the porosity of the metal foam can be calculated by

$$\varphi = 1 - \frac{\rho_{bulk}}{\rho_{metal}} \quad (1)$$

where $\varphi$ is the porosity and $\rho_{metal}$ is the density of the pure metal. The cell geometry of the metal foam is assumed to be the tetrakaidekahedron with cylinder ligaments and cubic nodes. With the thermal conductivity of the metal and oil known (copper 385 W/m·K, nickel 90 W/m·K, Krytox oil 0.0900 W/m·K and liquid R134a 0.0835 W/m·K (Haynes, 2014). It is known that the thermal conductivity of. The effective thermal conductivity of metal foam with/without oil-infused can be calculated using the classic three-dimensional foam model (Boomsma and Poulikakos, 2000), as listed in Table 1.

**Table 1:** The measured properties of the samples

| Type | Porosity (%) | Pore size (μm) | Thermal conductivity of lubricant-infused metal foam (W/m·K) | Thermal conductivity of liquid R134a infused metal foam (W/m·K) |
|---|---|---|---|---|
| Copper foam | 80.53±0.38 | 50 | 22.68 | 22.66 |
| Nickel foam | 77.07±0.24 | 40 | 6.70 | 6.68 |

### 3.2 Validation of the experimental conditions

In order to establish a confidence on the accuracy and repeatability of the condensation experiment, multiple parallel tests were conducted to compare the temperature profile and the internal vapor temperature and pressure variation. Having described the cold plate with two samples before, we used the nickel foam and copper for the validation of temperature measurement, as shown in Fig 4(a). TC-1 and TC-3 measured the temperature along the copper block with nickel foam, while TC-2 and TC-4 are with bare copper. The temperature curves showing consistency among the two parallel tests ensures the data accuracy and reproducibility. It was shown that the boundary condition is well controlled. The temperature curves dropped rapidly after the chiller circulation being connected and became stable in the first 5 minutes.

Fig 4(b) presents the pressure and vapor temperature change in five tests for two sets of samples: copper foam and bare copper; nickel foam and bare copper. Although the samples have different thermal properties, the results indicate a good agreement among the internal vapor state. The pressure slightly decreased at the initial condensation stage within 10%, because the heat flux was much higher with R134a vapor directly condensing on the cold solid surface. After the condensation became filmwise, the HTC decreased due to the thermal resistance of the condensate layer. Because the hot plate within the chamber served as a heat input, the pressure and vapor temperature gradually reached a steady stage.

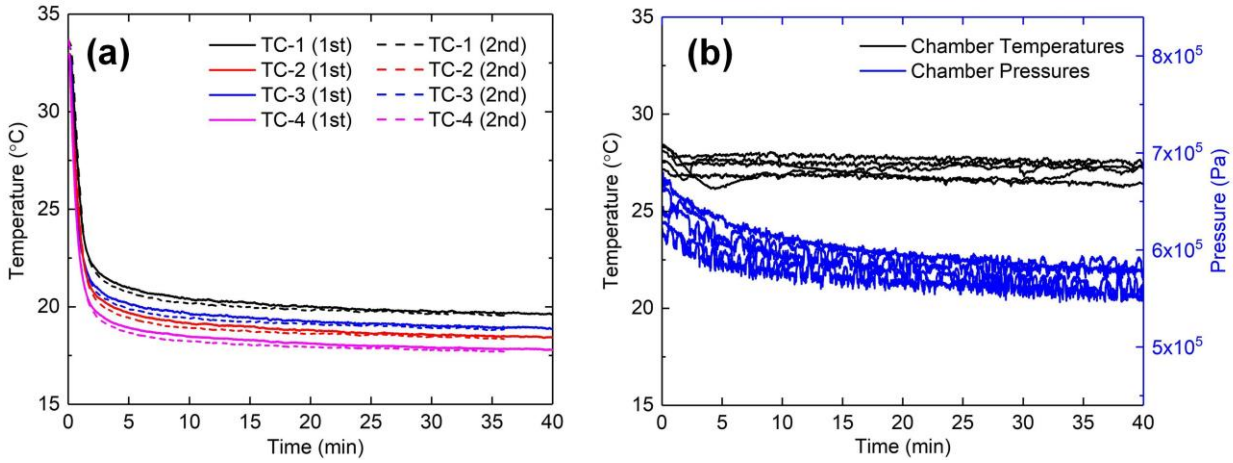


**Fig 4:** The measured (a) temperature variations by TCs, and (b) vapor temperatures and pressures in the chamber

### 3.3 Enhancement of condensation heat transfer

To investigate the influence of oil-infused metal foam on the R134a condensation heat transfer enhancement, the temperatures along the heat flux were measured, including the bottom surface of copper block $T_b$, the interface temperature between the sample and copper block $T_i$, and the vapor temperature $T_v$ (Fig 5). Since the thermal conductivity of copper block and metal foam samples are known, the heat flux can be calculated by

$$q = k_{Cu} \frac{T_i - T_b}{d_{Cu}} \tag{2}$$

where $k_{Cu}$ is the thermal conductivity of copper, $d$ is the thickness of the copper block. As we have determined the thermal conductivity of metal foams $k_{foam}$, the surface temperature would be

$$T_s = T_i + \frac{q \cdot d_{foam}}{k_{foam}} \tag{3}$$

where $d_{foam}$ is the thickness of the sample. Hence, the heat transfer coefficient $h$ could be determined by

$$h = \frac{q}{T_v - T_s} \tag{4}$$

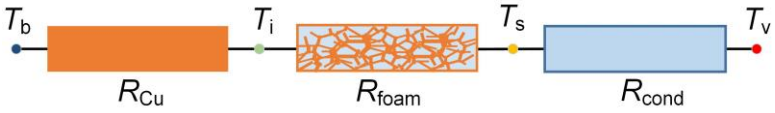


**Fig 5:** Schematic diagram showing the thermal resistance along the heat flux

As shown in Fig 6, the heat flux for two sets of samples have the same trend during condensation. The heat flux at the beginning has a sharp increase owing to the mechanisms of condensate nucleating and direct contact between vapor and solid surface. As the liquid film forming on the surface, the thermal resistance rapidly increases with the drop of heat flux. Afterwards, the condensate started to shed off from the surface due to gravity, which promote a small increase in heat transfer. Approaching the steady filmwise condensation region, the heat flux settled at 15~20 kW/m$^2$. The value of heat flux through the metal foams and copper are close, while the former is higher. Multiple parallel tests were conducted to validate the accuracy and repeatability of the data.

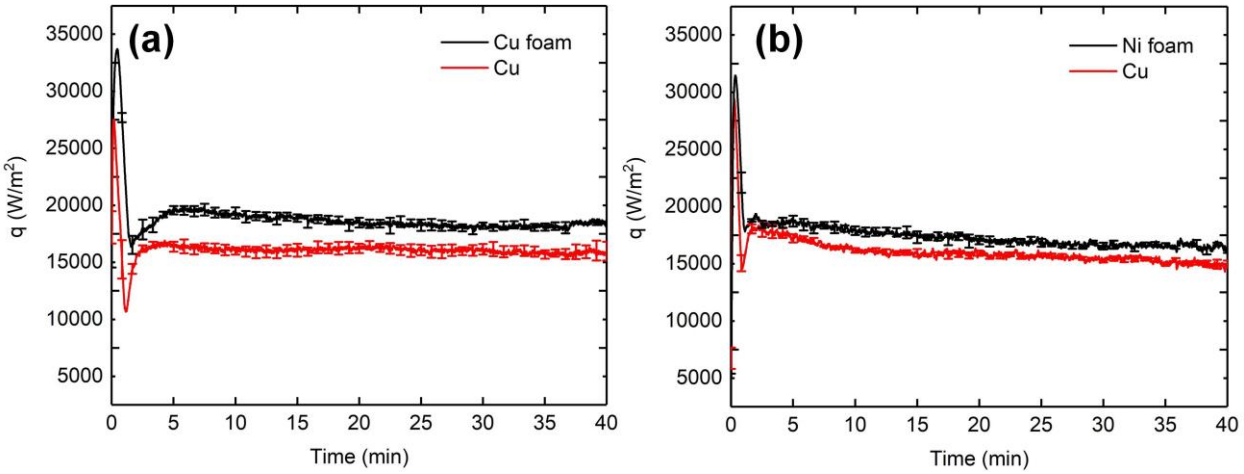


**Fig 6:** Heat flux over time during condensation for (a) copper foams and (b) nickel foams versus bare copper

As presented in Fig 7, the heat transfer coefficients of oil-infused and empty metal foams are compared with bare copper samples. The HTC is very large at the beginning of condensation, which agrees with the heat flux variation. Noted that HTC of the metal foam are always higher than bare copper surface. Because of the immiscibility of Krytox 1506 to R134a, the oil-infused metal foams surface shows repellence to the condensate. This repellence promotes the liquid shedding more quickly from the sample surface than regular metal. We also investigate the performance of empty metal foams in hear transfer enhancement. The HTC for the metal foam without oil is still increased compared to copper, which could be understood by the larger surface area.

In addition, the HTC degrading from the oil-infused to empty metal foams can be explained by noting that the lubricant oil was depleted by the shedding condensate of R134a. The different drop of HTC between nickel and copper foam stems from their ability of holding oil. The micro-scale pores within metal foams, as presented in Fig 1, have different structures by metal powder sintering, although the pore sizes are similar. The nickel foam has an ink bottle shape, and the copper foam have the network structure, showing the metal ligaments with junctions. Hence, the nickel foam locked the lubricant oil with capillary force for a longer time than copper foams, and also resulted in a better enhancement of condensation heat transfer. However, there are still limits in maintaining oil within the

porous structure. The shear force of film condensate breaking down would also carry the oil with them, especially during the condensation at a high heat flux.

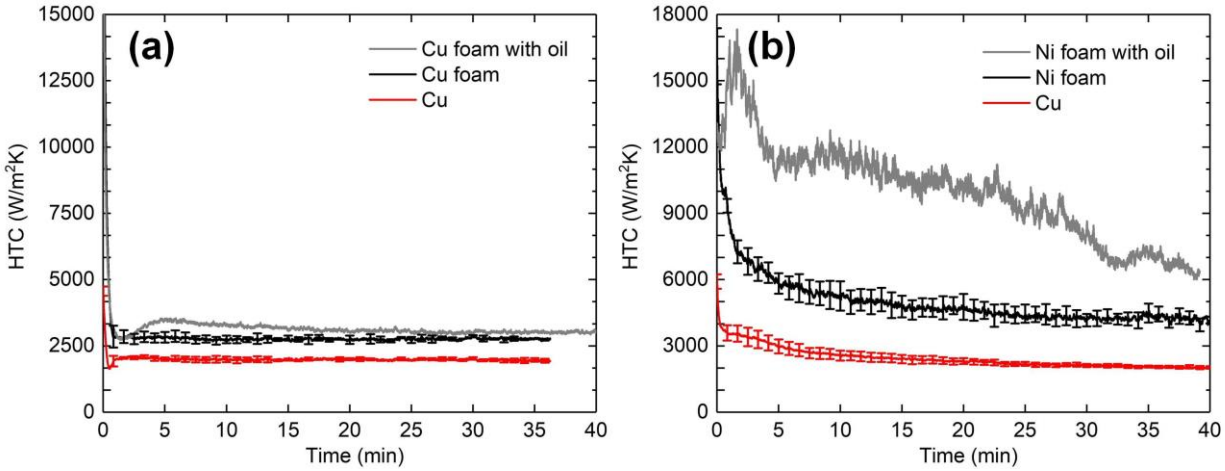


**Fig 7:** HTC over time during for (a) oil-infused and empty copper foams, and (b) nickel foams versus pure copper

## 4. CONCLUSIONS

In this paper, we experimentally studied the R134a condensation heat transfer on oil-infused metal foams under saturation state. It was demonstrated that the heat transfer coefficient on metal foams was higher than pure copper. Having discussed the mechanism of condensation process by applying metal foams, we demonstrate some concluding remarks as follows:

- The accuracy and repeatability of the condensation experiment were validated by the consistency among temperature profile and the internal vapor temperature and pressure variation via multiple parallel tests.
- The heat flux at steady filmwise condensation settled at 15~20 kW/m$^2$. The value of heat flux through the metal foams and copper are close, while the former is higher.
- Compare to the pure copper surface, the heat transfer coefficient of the oil-infused metal foam increases by 102% for nickel foam and 53% for copper foam at steady condensation state.

## NOMENCLATURE

The nomenclature should be located at the end of the text using the following format:

| | | |
|---|---|---|
| $T$ | temperature | (°C) |
| $h$ | heat transfer coefficient | (W/m$^2$·K) |
| $q$ | heat flux | (W/m$^2$) |
| $d$ | length along heat flux | (m) |
| $k$ | thermal conductivity | (W/m·K) |
| $\rho$ | density | (kg/m$^3$) |
| $\varphi$ | porosity | (%) |

**Subscript**

| | |
|---|---|
| b | bottom surface |
| i | interface |
| s | surface |
| v | vapor` |

## REFERENCES

Boomsma, K., & Poulikakos, D. (2001). On the effective thermal conductivity of a three-dimensionally structured fluid-saturated metal foam. *Int. J. Heat Mass Transfer*, *44*(4), 827-836.

Chen, X., Wu, J., Ma, R., Hua, M., Koratkar, N., Yao, S., & Wang, Z. (2011). Nanograssed micropyramidal architectures for continuous dropwise condensation. *Adv. Funct. Mater.*, *21*(24), 4617-4623.

Gebauer, T., Al-Badri, A. R., Gotterbarm, A., El Hajal, J., Leipertz, A., & Fröba, A. P. (2013). Condensation heat transfer on single horizontal smooth and finned tubes and tube bundles for R134a and propane. *Int. J. Heat Mass Transfer*, *56*(1-2), 516-524.

Haynes, W. M. (Ed.). (2014). *CRC handbook of chemistry and physics*. CRC press.

Hu, H. W., & Tang, G. H. (2014). Theoretical investigation of stable dropwise condensation heat transfer on a horizontal tube. *Appl. Therm. Eng.*, *62*(2), 671-679.

Li, X. M., Reinhoudt, D., & Crego-Calama, M. (2007). What do we need for a superhydrophobic surface? A review on the recent progress in the preparation of superhydrophobic surfaces. *Chem. Soc. Rev.*, *36*(8), 1350-1368.

Li, J., & Hrnjak, P. (2017). Improvement of condenser performance by phase separation confirmed experimentally and by modeling. *Int. J. Refrigeration*, *78*, 60-69.

Lu, T. J., Stone, H. A., & Ashby, M. F. (1998). Heat transfer in open-cell metal foams. *Acta Mater.*, *46*(10), 3619-3635.

Miljkovic, N., & Wang, E. N. (2013). Condensation heat transfer on superhydrophobic surfaces. *MRS Bull.*, *38*(5), 397-406.

Preston, D.J., Lu, Z., Song, Y., Zhao, Y., Wilke, K.L., Antao, D.S., Louis, M., & Wang, E.N. (2018). Heat transfer enhancement during water and hydrocarbon condensation on lubricant infused surfaces. *Sci. Rep.*, *8*(1), 540.

Rahman, M. A., & Jacobi, A. M. (2013). Condensation, frost formation, and frost melt-water retention characteristics on microgrooved brass surfaces under natural convection. *Heat Transfer Eng.*, *34*(14), 1147-1155.

Rose, J. W. (2004). Surface tension effects and enhancement of condensation heat transfer. *Chem. Eng. Res. Des.*, *82*(4), 419-429.

Rykaczewski, K., Paxson, A.T., Staymates, M., Walker, M.L., Sun, X., Anand, S., Srinivasan, S., McKinley, G.H., Chinn, J., Scott, J.H.J. and Varanasi, K.K. (2014). Dropwise condensation of low surface tension fluids on omniphobic surfaces. *Sci. Rep.*, *4*, 4158.

Sett, S., Yan, X., Barac, G., Bolton, L. W. and Miljkovic, N. (2017). Lubricant-infused surfaces for low-surface-tension fluids: promise versus reality. *ACS. Appl. Mater. Inter.*, *9*(41), 36400-36408.

Vemuri, S. and Kim, K.J. (2006). An experimental and theoretical study on the concept of dropwise condensation. *Int. J. Heat Mass Transfer*, *49*(3-4), 649-657.

Vogel, N., Belisle, R. A., Hatton, B., Wong, T. S. and Aizenberg, J. (2013). Transparency and damage tolerance of patternable omniphobic lubricated surfaces based on inverse colloidal monolayers. *Nat. Commun.*, *4*, 2176.

Webb, R. L. (1988). Enhancement of film condensation. *Int. Commun. Heat Mass*, *15*(4), 475-507.

Wen, R., Xu, S., Ma, X., Lee, Y. C. and Yang, R. (2017). Three-dimensional superhydrophobic nanowire networks for enhancing condensation heat transfer. *Joule*.

Xiao, L., Li, J., Mieszkin, S., Di Fino, A., Clare, A.S., Callow, M.E., Callow, J.A., Grunze, M., Rosenhahn, A. and Levkin, P.A. (2013). Slippery liquid-infused porous surfaces showing marine antibiofouling properties. *ACS. Appl. Mater. Inter.*, *5*(20), 10074-10080.

Yu, R., & Jacobi, A. M. (2015). Water-repellent slippery surfaces for HVAC&R systems. In *ASME 2015 Conference on Smart Materials, Adaptive Structures and Intelligent Systems* (pp. V001T01A019-V001T01A019). American Society of Mechanical Engineers.

## ACKNOWLEDGEMENT

The work is supported by the Air Conditioning and Refrigeration Center (ACRC) and Zhejiang University - University of Illinois at Urbana Champaign (ZJU-UIUC) Institute Research Program.